ACS OMEGA

Article

Cite This: ACS Omega 2018, 3, 3420−3428

Self-Assembly of Graphene-Encapsulated Cu Composites for Nonenzymatic Glucose Sensing

Qi Zhang,[†,‡] Qin Luo,[†,‡] Zhenbo Qin,[†,‡] Lei Liu,[*,†,‡] Zhong Wu,[*,§] Bin Shen,[†,‡] and Wenbin Hu[§]

[†]State Key Laboratory of Metal Matrix Composites, School of Materials Science and Engineering, Shanghai Jiao Tong University, Shanghai 200240, China

[‡]Collaborative Innovation Center for Advanced Ship and Deep-Sea Exploration, Shanghai 200240, China

[§]Tianjin Key Laboratory of Composite and Functional Materials, School of Materials Science and Engineering, Tianjin University, Tianjin 300072, China

Supporting Information

ABSTRACT: Cu has recently received great interest as a potential candidate for glucose sensing to overcome the problems with noble metals. In this work, reduced graphene oxide-encapsulated Cu nanoparticles (Cu@RGO) have been prepared via an electrostatic self-assembly method. This core/shell composites were found to be more stable than conventional Cu-decorated graphene composites and bare copper nanoparticles in an air atmosphere because the graphene shell can effectively protect the Cu nanoparticles from oxidation. In addition, the obtained Cu@RGO composites also showed an outstanding electrocatalytic activity toward glucose oxidation with a wide linear detection range of 1 μM to 2 mM, low detection limit of 0.34 μM (S/N = 3), and a sensitivity of 150 μA mM^{-1} cm^{-2}. Moreover, Cu@RGO composites exhibited a satisfactory reproducibility, selectivity, and long effective performance. These excellent properties indicated that Cu@RGO nanoparticles have great potential application in glucose detection.

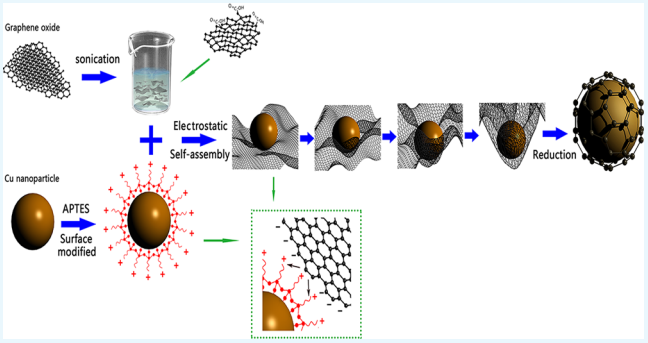

1. INTRODUCTION

Diabetes, a worldwide public chronic disease, which is related to high levels of glucose in the blood, has affected millions of people during the past decades.[1,2] In this regard, the development of fast and reliable methods for glucose detection is quite important in many areas, such as clinical diagnostics and food and medicine industry.[3] Among them, electrochemical detection techniques were applied universally for glucose detection due to their high sensitivity, stability, simple instrumentation, and low cost.[4−7] Generally, electrochemical glucose sensors can be divided into two types: enzymatic and nonenzymatic. However, the enzymatic glucose sensors have several inevitable disadvantages because of the intrinsic nature of the enzyme, such as insufficient long-term stability, high cost, and poor electrical conductivity.[8,9] Moreover, the activity of enzymes is susceptible to environmental factors (such as temperature, pH value, and toxic chemicals).[10] Therefore, nonenzyme-based glucose biosensors have become a hot research topic in these years.

Recently, noble metal nanoparticles (such as silver, gold, and platinum), due to their unique catalytic activity, have attracted a great deal of attention as nonenzymatic electrode materials in the area of glucose sensors. However, noble materials were usually scarce and expensive for commercial use and easily poisoned during the experimental processes, which limited their widespread electrocatalytic applications.[11−13] Therefore, replacement of noble metals with other cheaper materials is of great importance in the field of biosensing application. Recently, Cu nanoparticles were emerging as a new promising electrode material for the detection of glucose and many research groups have investigated their electrocatalyst ability.[3,14,15] However, bare Cu nanoparticles in the air atmosphere easily suffered from oxidation within several hours and therefore hampering their long-term commercial practice.[11,16] Moreover, our previous research indicated a molecular-level mixing process to fabricate Cu-decorated reduced graphene oxide (RGO/Cu) composites and investigated their electrocatalytic performance for glucose detection.[17] However, some papers indicated that the bare metal particles on the graphene layer were also unstable in harsh conditions after a period of time.[18]

Fortunately, the core−shell structure can effectively immunize the encapsulated nanomaterial against environment degradation effects.[11] Compared with other coatings (organic molecules, polymers, or oxides), carbon coating has many advantages due to its higher electron transportations and

Received: August 17, 2017
Accepted: October 10, 2017
Published: March 23, 2018

DOI: 10.1021/acsomega.7b01197
ACS Omega 2018, 3, 3420−3428

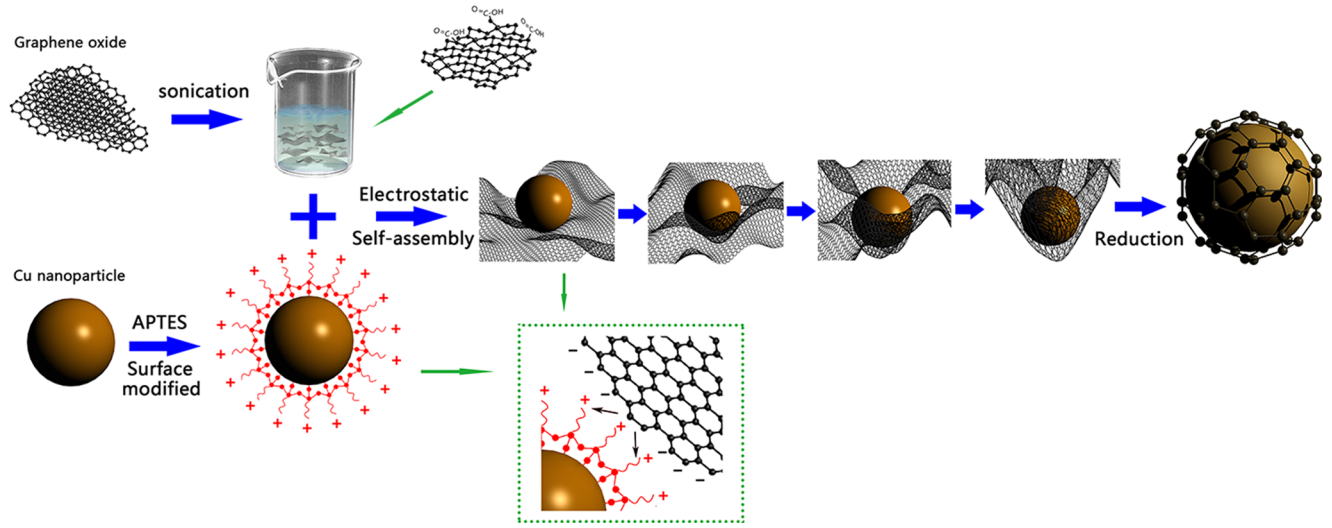

Figure 1. Schematic illustration of the synthesis route for graphene-encapsulated Cu nanoparticles.

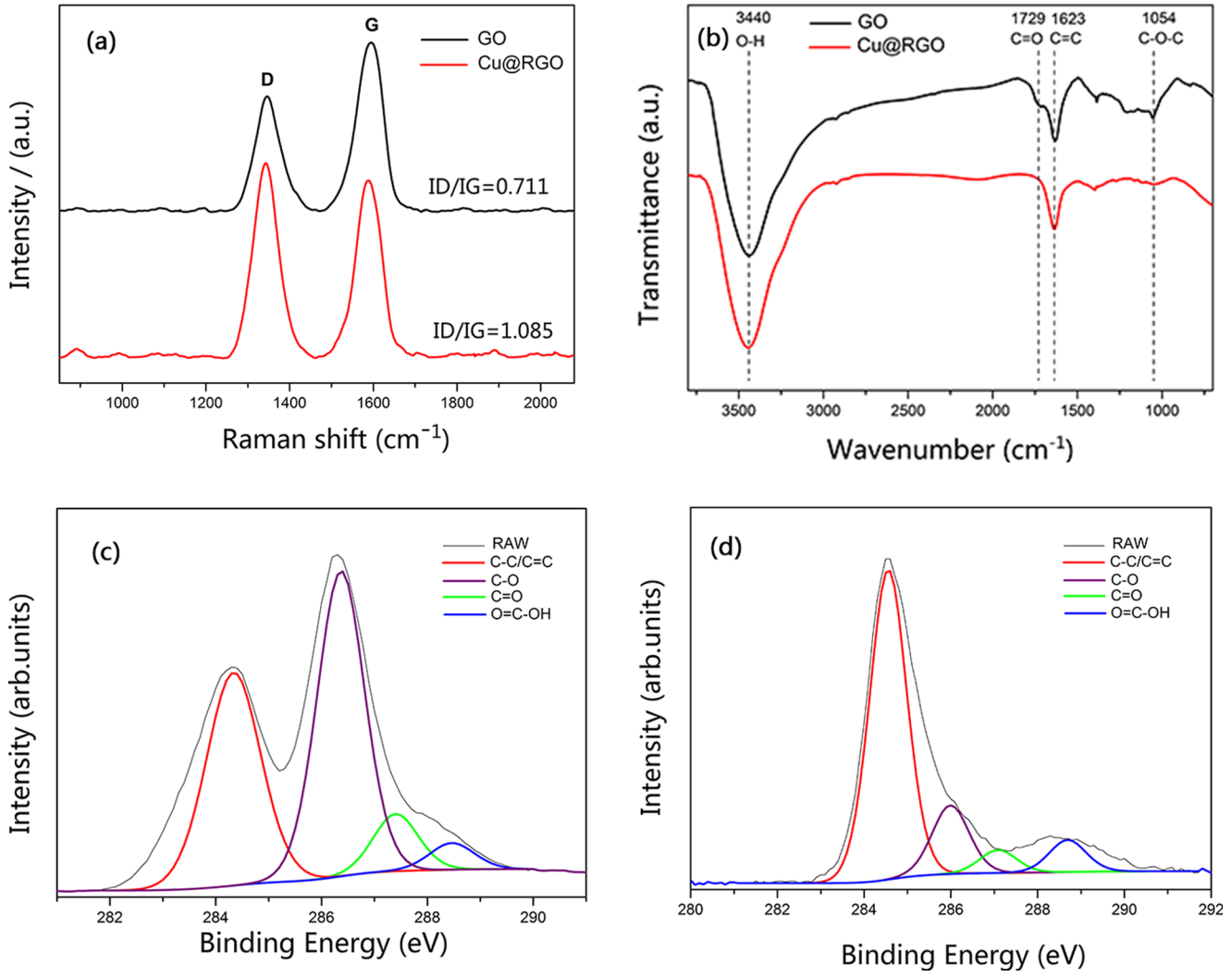

Figure 2. (a) Raman spectra and (b) Fourier transform infrared (FTIR) spectra of GO and Cu@RGO. Deconvoluted high-resolution C 1s X-ray photoelectron spectroscopy (XPS) spectra of (c) GO and (d) Cu@RGO.

chemical and thermal stability.[19−21] Graphene, as a two-dimensional single-layer carbon sheet, has attracted great interest to be used as a coating material for electrocatalytic applications because of large specific surface area, extraordinary carrier transport mobility, and excellent chemical stability.[22−24] Actually, the flexible graphene can not only prevent the volume

DOI: 10.1021/acsomega.7b01197
ACS Omega 2018, 3, 3420−3428

expansion/contraction of nanoparticles but also improve the catalytic performance due to the strong synergistic interaction between the two components and electrical conductivity of the overall electrode.[18,20] Until now, graphene-encapsulated metal nanoparticles have been widely studied in electrochemical applications. For example, Hang et al. fabricated Cu@RGO core/shell nanostructure arrays using monolayer colloidal crystals as templates, which exhibited efficient catalytic activity in the reduction of 4-NP to 4-AP.[25] Wang et al. prepared graphene-encapsulated nickel nanoparticles, which showed excellent catalytic performance for the methanation reaction.[26]

In this work, we presented a facile strategy to fabricate graphene-encapsulated Cu nanoparticles by electrostatic self-assembly. It is the first time when an electrostatic self-assembly route is developed for the fabrication of composites of Cu nanoparticles encapsulated in graphene shells and then their electrocatalytic activity is systemically investigated toward the oxidation of glucose. Moreover, the experimental process for the synthesis of graphene-encapsulated Cu nanoparticles in our case was simple and was carried out without using complicated and expensive equipment. Generally, electrostatic self-assembly is based on the principle of electrostatic attraction between two oppositely charged particles suspended in the solution.[27] The individual Cu nanoparticle surfaces were first modified with 3-aminoprooyltriethoxysilane (APTES) to render the surface positively charged and then encapsulated by negatively charged graphene oxide (GO) sheets because there were abundant oxygen-containing functional groups (such as carboxyl, epoxy, and hydroxyl) on the GO sheets. After reduction by sodium hypophosphite monohydrate ($NaH_2PO_2{\cdot}H_2O$), self-assembled graphene-encapsulated Cu composites (Cu@RGO) were achieved. The high-resolution transmission electron microscopy (HRTEM) image also verified that there were few-layer graphene sheets covering the surface of Cu nanoparticles. Moreover, these as-prepared Cu@RGO nanoparticles exhibited excellent catalytic activity for glucose and air stability than those of bare Cu and RGO/Cu composites even after 30 days, showing a great potential as high-efficiency materials in the field of glucose sensors.

2. RESULTS AND DISCUSSION

2.1. Characterizations of Structures and Morphologies. Figure 1 shows the schematic illustration of the synthesis of Cu@RGO composites by the electrostatic self-assembly method. More details can be seen in the Methods section. The atomic force microscopy (AFM) image of the as-prepared GO sheets can be seen in Figure S1a (Supporting Information). It can be seen that GO sheets have not overlapped, and the height profile diagram showed that the thickness of GO was 0.88 nm, which was consistent with the typical thickness of a single-layer GO.[28] Figure S1c,d shows the scanning electron microscopy (SEM) and transmission electron microscopy (TEM) images of GO sheets. It can be seen that GO has a paperlike structure with corrugations and ripples. The inset of Figure S1c shows a digital photo of the GO solution. Combined with the results of AFM, indicating that the most of GO in this work was efficiently exfoliated. Moreover, the distribution of GO is shown in Figure S2 and the average size of GO was 858 nm.

Figure 2a shows the Raman spectra of GO and Cu@RGO. Two bands were observed at 1347 and 1595 cm^{-1} for GO. The former was called the D band, which corresponded to the A_{1g} phonon of sp^3 carbon atoms of the disordered graphite. The latter was called the G band, which originated from the in-plane vibration of sp^2 carbon atoms.[29,30] After reduction, the D band and G band shifted to 1342 and 1585 cm^{-1}, respectively, indicating the recovery of the hexagonal network of the carbon atom in graphene.[31] Furthermore, the change of the relative intensities of the D and G bands (ID/IG) provided the information of the amount of structure defects and a quantitative measure of the edge plane exposure.[32] In our case, this ratio has been found to increase from 0.711 (GO) to 1.085 (Cu@RGO), indicating the decrease in the size of the in-plane sp^2 domains and the partially ordered crystal structure of graphene sheets.[33]

Figure 2b shows the FTIR spectra of GO and Cu@RGO composites. In the spectrum of GO, the typical peaks were as follows: 3440 and 1729 cm^{-1}, which correspond to O−H stretching vibrations of C−OH groups and C═O stretching vibrations from carbonyl groups. The two peaks at 1623 and 1054 cm^{-1} were assigned to the C═C configurable vibrations from aromatic zooms and C−O vibrations from alkoxy groups.[34] For the Cu@RGO composites, the peak positions of the functional groups on GO still remained, but the intensities of C═O and C−O decreased drastically, whereas the intensity of C═C was much stronger than that on GO. These changes proved that most of the oxygen-containing functional groups on GO have been successfully removed.

Moreover, XPS was employed to further analyze the reduction degree of Cu@RGO. The deconvoluted XPS C 1s spectra of GO (Figure 2c) exhibited four components: C−C/C═C (284.9 eV), C−O (286.5 eV), C═O (287.1 eV), and O═C−OH (288.9 eV). However, the XPS C 1s spectrum of Cu@RGO (Figure 2d) was clearly different from that of GO and the peak intensities of oxygen-containing groups decreased significantly. Specifically, the peak area ratios of the C−O, C═O, and O═C−OH bonds to C−C/C═C of GO were 1.245, 0.221, and 0.103, and the corresponding ratios for Cu@RGO were 0.041, 0.018, and 0.045, respectively. This result indicated that the oxygenated groups on the surface of GO sheets have been reduced.

The air stability of Cu@RGO can be identified by X-ray diffraction (XRD) and TEM. Figure 3 shows the XRD results of pure Cu, RGO/Cu, and Cu@RGO composites for 30 days (the samples were denoted Cu@RGO-30, RGO/Cu-30, and

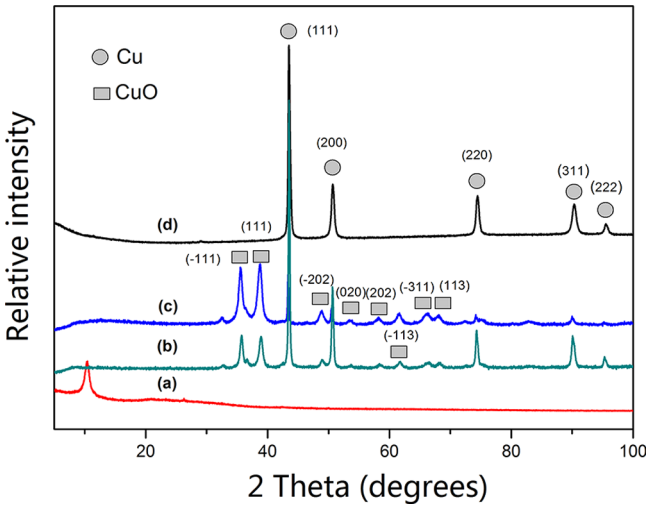

Figure 3. XRD patterns of (a) GO, (b) pure Cu, (c) RGO/Cu composites, and (d) Cu@RGO composites.

DOI: 10.1021/acsomega.7b01197
ACS Omega 2018, 3, 3420−3428

pure Cu-30, respectively). Compared to those for pure Cu and RGO@Cu composites, no peaks of copper oxides can be seen for Cu@RGO composites, and there were five reflection peaks located at 43.28, 50.88, 74.45, 89.72, and 95.26°, which can be assigned to Cu (111), Cu (200), Cu (220), Cu (311), and Cu (222) (JCPDS No. 65-9026), respectively. Obviously, Cu@RGO has a better oxidation resistance than that of pure Cu and RGO/Cu composites because the graphene shell could act as a shield to prevent the metal core from oxidation.[16,35] Additionally, the peak of RGO (26°) has not been found in the Cu@RGO samples. This can be ascribed to the small loading of RGO in the composite and the low scattering length of carbon compared to that of copper atoms.[36]

Figure 4a displays the low-magnification TEM image of Cu@RGO nanoparticles, which showed a typical core−shell

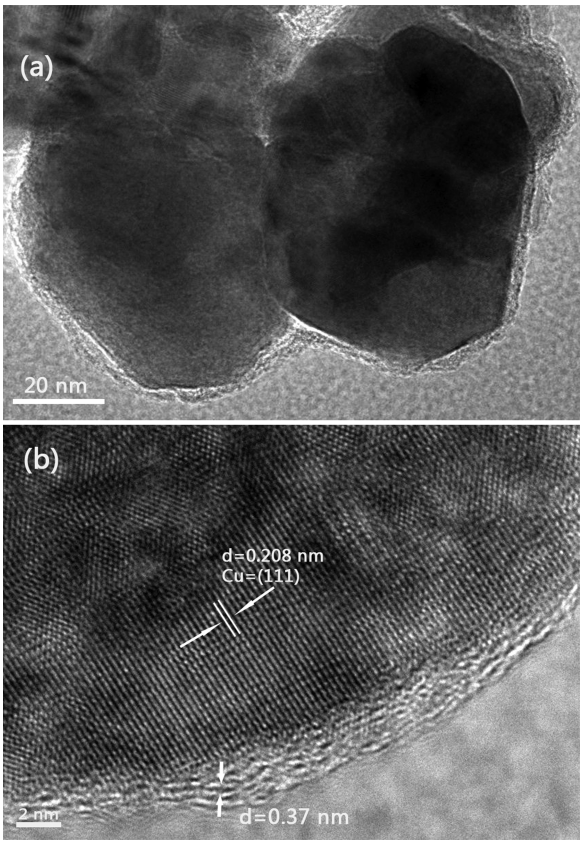

Figure 4. (a) Low-magnification and (b) high-magnification TEM images of the Cu@RGO composites.

structure due to the Cu core encapsulated by a graphene shell. Figure 4b shows the corresponding HRTEM image and exhibited that the Cu core still has a great crystalline structure under the protection of the few-layer graphene shell. The lattice spacing of Cu was 0.208 nm, which was in accordance with the *d*-spacing of the (111) plane of the Cu crystal. Furthermore, it can be seen that the lattice spacing of the graphene shell was 0.37 nm, which can be indexed to the {0002} planes of graphite.[37]

2.2. Electrochemical Measurements. To compare the catalytic activity more effectively, the particle sizes of the referential pure Cu, RGO/Cu, and Cu@RGO composites (Figure 5) used in this electrochemical characterization were similar (≈40 nm). As shown in Figure 6a, the electrochemical activity was investigated by cyclic voltammetry (CV) in 0.1 M NaOH without addition of glucose. Apparently, no oxidation peak existed in the absence of glucose, which means that all of the samples have some electrocatalytic effect in the NaOH solution. Moreover, Figure 6b shows that some oxidation peaks appeared in all of the samples in the case of glucose. Among all of the samples, the Cu@RGO composite had the highest peak current for glucose oxidation and the pure Cu had the weakest, indicating that Cu@RGO had the better catalytic activity than that of RGO/Cu and pure Cu specimens. The higher electrocatalytic activity of Cu@RGO can be ascribed to the synergistic effect of Cu and graphene. This core/shell structure increased the contact surface area between the Cu core and graphene shell because the Cu core was wrapped all around by the graphene, which acted as a continuous path for rapid electron transport.[38] Moreover, the carrier transport efficiency could also be improved significantly, arising from graphene encapsulation.[22,39]

Additionally, the long-term storage and stability of the modified electrodes were crucial for the continuous monitoring of glucose in practical applications. After exposure to air environment for 30 days, all of the samples (Cu@RGO, RGO/Cu, and pure Cu) exhibited different electrocatalytic performance toward glucose. Apparently, the Cu@RGO-30 composites still retained excellent catalytic activity, indicating that few-layer graphene-encapsulated Cu had great long-term stability because graphene shells could effectively protect Cu cores from oxidation while retaining their intrinsic catalytic properties. Conversely, the electrochemical performance of RGO/Cu-30 and pure Cu-30 decreased significantly due to the parts of Cu nanoparticles being oxidized to form CuO within these days, which can be observed in Figure 3. Moreover, it could be seen that RGO/Cu-30 had better catalytic activity than that of pure Cu-30. This was attributed to the functional groups on the surface of GO, offering the anchoring points for metal nanoparticles. In addition, some Cu nanoparticles were covered with graphene sheets and therefore saved from oxidation.

Figure S3 illustrates the mechanism for the oxidation of glucose in the NaOH solution at the as-prepared Cu@RGO composite electrode.[40−42] First, Cu nanoparticles can be electrochemically oxidized into Cu(II) (CuO and $Cu(OH)_2$) in alkaline media.

$$Cu + 2OH^- \rightarrow CuO + H_2O + 2e^- \quad (1)$$

or

$$Cu + 2OH^- \rightarrow Cu(OH)_2 + H_2O + 2e^- \quad (2)$$

Second, CuO is oxidized to a strong oxidizing agent of the Cu(III) species ($CuOOH^-$ or $Cu(OH)_4^-$).

$$CuO + OH^- \rightarrow CuOOH + e^- \quad (3)$$

or

$$CuO + H_2O + 2OH^- \rightarrow Cu(OH)_4^- + e^- \quad (4)$$

Finally, glucose was catalytically oxidized by the Cu(III) species and formed hydrolyzate gluconic acid.

$$Cu(III) + \text{glucose} \rightarrow \text{gluconolactone} + Cu(II) \quad (5)$$

$$\text{gluconolactone} \rightarrow \text{gluconic acid (hydrolysis)} \quad (6)$$

Differential pulse voltammetry (DPV) was performed as a more sensitive voltammetric technique to investigate the dependence of peak current on the concentration of glucose. Before recording the DPV voltammograms, moderate stirring was

DOI: 10.1021/acsomega.7b01197
ACS Omega 2018, 3, 3420−3428

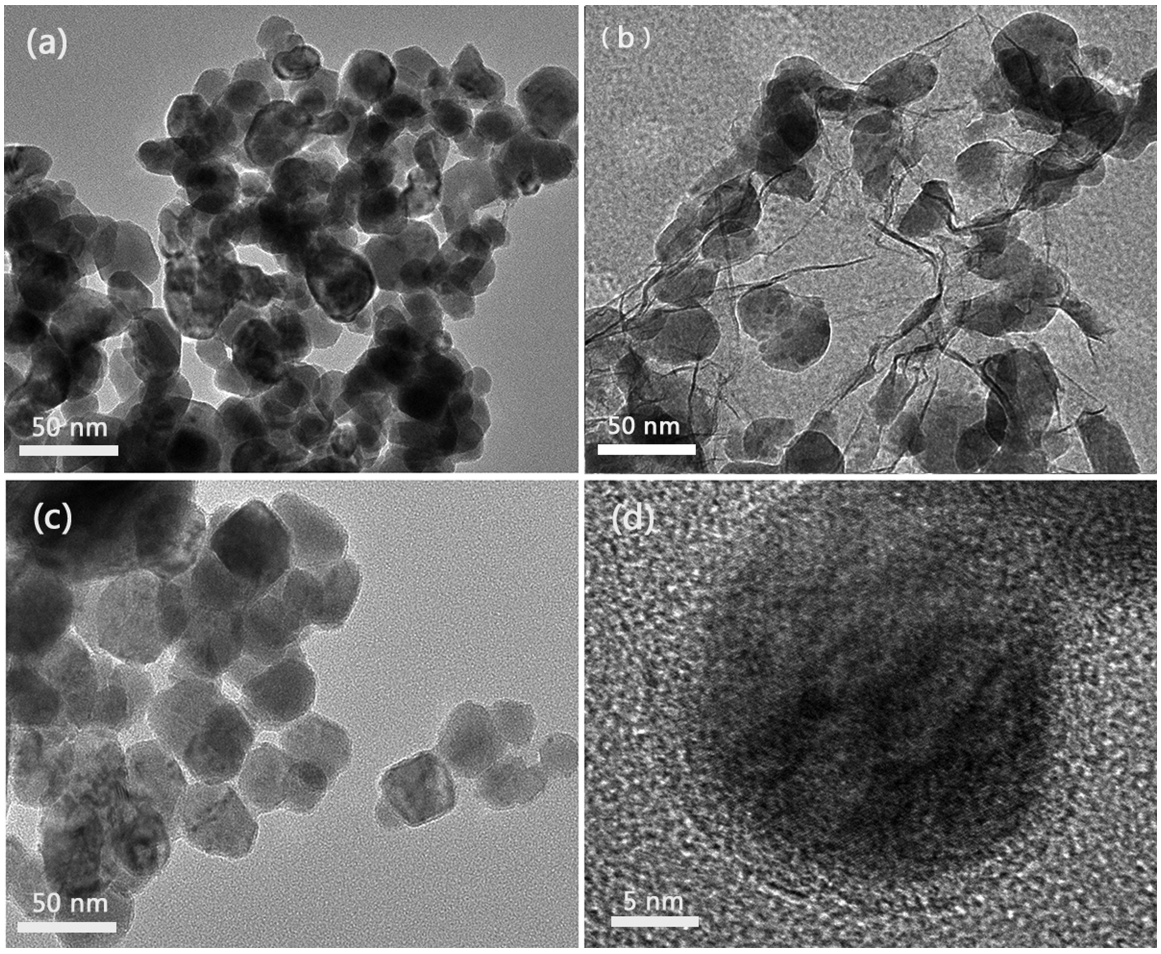

Figure 5. TEM images of (a) pure Cu, (b) RGO/Cu, and (c, d) Cu@RGO composites. The HRTEM image of graphene shells around the Cu nanoparticles can be seen in (d).

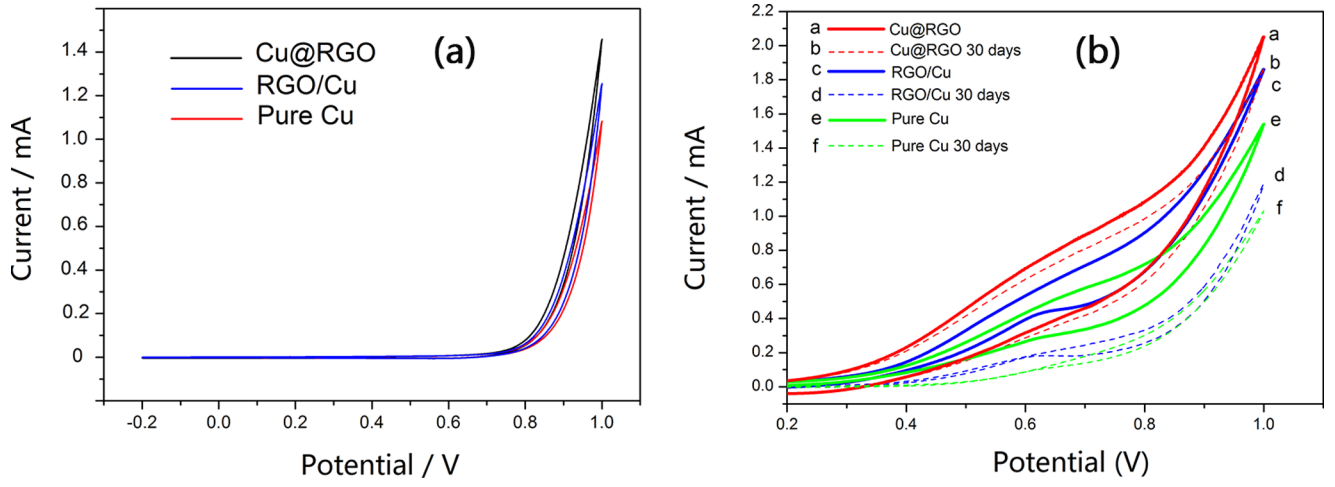

Figure 6. CV curves of (a) Cu@RGO, RGO/Cu, and pure Cu samples in the absence of glucose in 0.1 M NaOH solution and (b) Cu@RGO, RGO/Cu, pure Cu, Cu@RGO-30 days, RGO/Cu-30 days, and pure Cu-30 days in the presence of 2 mM glucose in 0.1 M NaOH.

continued for about 5 min when glucose was added. Figure 7a shows a typical DPV voltammogram of various concentrations of glucose at the Cu@RGO-modified electrodes in 0.1 M NaOH solution. Obviously, the current responses increased linearly with glucose concentrations in the range of 1 μM−2 mM with a current sensitivity of 150 μA mM^{-1} cm^{-2} (Figure 7b). The corresponding regression equation could be described as follows: $y = 76.84 + 0.132C_{glucose}$ ($R^2 = 0.992$). The detection limit of the method was determined to be 0.34 μM with the signal-to-noise (S/N) ratio of 3. Moreover, the effective surface area of Cu@RGO electrocatalysts can be determined by CV. Figure S4 shows the CV curves of the obtained Cu@RGO composites in 0.1 M N_2-saturated NaOH solution, and the effective surface area was estimated to be 16.81 cm^2. For

DOI: 10.1021/acsomega.7b01197
ACS Omega 2018, 3, 3420−3428

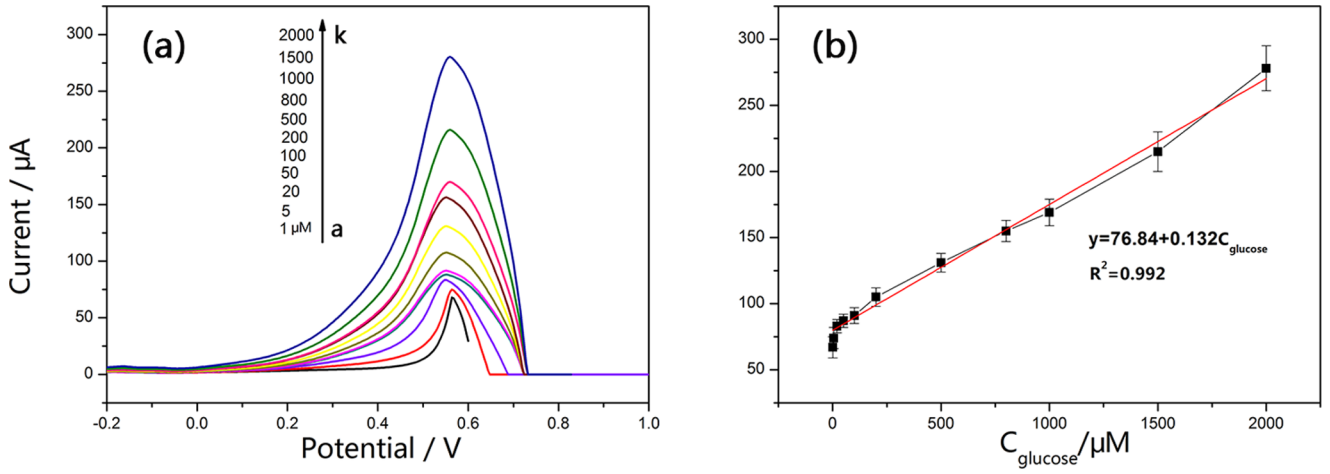

Figure 7. (a) Differential pulse voltammogram responses of the graphene-encapsulated Cu composites in different concentrations (from a to k: 1, 5, 20, 50, 100, 200, 500, 800, 1000, 1500, and 2000 μM) of glucose in 0.1 M NaOH. (b) Linear relationship between the peak current and the analyte concentration.

Table 1. Comparison of the Cu@RGO Electrode with Other Previously Reported Nonenzymatic Glucose Sensors Based on Cu Nanomaterials

electrode materials	sensitivity (μA mM^{-1} cm^{-2})	linear range (mM)	LOD (μM)	references
CuNP/RGO	447.65	0.01−1.2	3.4	46
CuNP/graphene glassy carbon electrodes (GCE)	607	0.005−1.4	0.2	47
CuO nanorods/graphite	371.43	0.004−8	4.0	48
CuNP/GO/single-walled carbon nanotubes	930.07	0.001−4.538	0.34	44
Cu foam	3581.1	0.18−3.47	12.3	49
Cu	1096	up to 7.5	1	50
Cu/graphene		4.5	0.5	51
Cu-CNTs	17.76	0.0007−3.5	0.21	52
CuNPS/multi-walled carbon nanotubes (MWCNTs)	50.47	0.01−0.3	0.5	53
Cu nanowires-MWCNTs	1995	up to 3	5	54
Cu-N-G	48.13	0.004−4.5	1.3	45
CuNiNPs-3D-KSCs	19.16	0.007−23.67	2.3	6
CuO nanowire	490	0.0004−2	0.049	55
Ag/CuO	1347	0.0005−0.5	0.057	56
Cu@RGO	150	0.001−2	0.34	this work

comparison, the performances of the as-prepared Cu@RGO and other previously reported nonenzymatic glucose sensors based on Cu have been listed in Table 1. As presented in Table 1, the developed Cu@RGO composites exhibited great sensitivity and limit of determination (LOD) of glucose sensing among these electrodes. The higher catalytic activity of as-prepared Cu@RGO core/shell nanoparticles originated from the synergistic effect between Cu nanoparticles and RGO, which has large specific surface area (2600 m^2 g^{-1}) and extraordinary electron transport properties.[43] Besides that, the copper particle size in our case was relatively small than that in some reports.[44,45] It is well known that the nanoparticles with a smaller size have a higher catalytic activity due to larger active surface areas.[25]

The reproducibility of Cu@RGO composites was investigated from the voltammetric response of 2 mM glucose for successive measurements at the same 10 modified electrodes, which were prepared using the same electrostatic self-assembly method. A relative standard deviation of 4.2% was obtained toward 2 mM glucose, confirming an excellent reproducibility of the fabricated electrode.

Apart from reproducibility and stability, selectivity was also an important feature for glucose detection. In real serum samples, several electroactive substances, such as dopamine (DA), L-ascorbic acid (AA), and uric acid (UA), usually coexisted with glucose and interfered the detection of glucose. Therefore, in our experiments, the selectivity of Cu@RGO was evaluated via DPV with the addition of 1 mM glucose in 0.1 M NaOH in the absence and presence of possible interferences (AA, DA, and UA) for the detection of glucose. Figure 8 exhibits the exact contrast among the above interferences, which was calculated by normalizing the current responses of the Cu@RGO composites upon 1 mM glucose and was 100%. Instead of adding glucose, each interference (2 mM AA, DA, and UA) was separately added, and the corresponding DPV current decreased lightly occupied only 6.3, 8.9 and 5.4% of which originated from 1.0 mM glucose, respectively. It could be seen that the signal intensities after adding these interferences to the glucose solution were kept nearly constant in the presence of interference, proving that the Cu@RGO electrode had a great selectivity.

To verify the possibility of practical application, the obtained Cu@RGO nanocomposites in this work were applied to determine glucose in human blood serum samples. Specifically, 30 μL of the blood sample was added to 30 mL of 0.1 M NaOH solution, and the optimal detection potential of 0.6 V

DOI: 10.1021/acsomega.7b01197
ACS Omega 2018, 3, 3420−3428

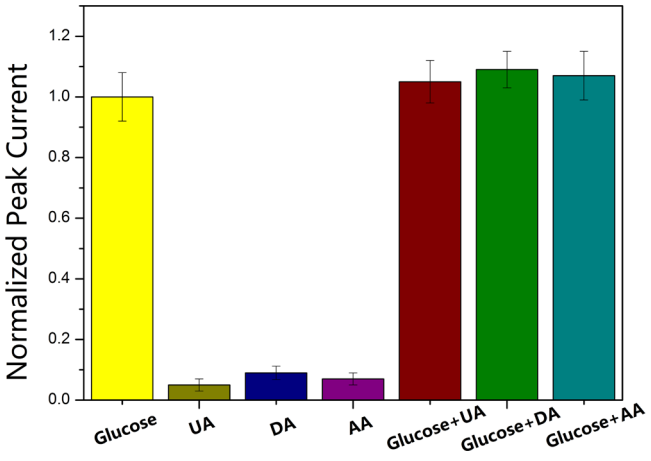

Figure 8. Normalized DPV peak current changes of Cu@RGO composites with the respective addition of 1.0 mM glucose, 2.0 mM UA, 2.0 mM DA, 2.0 mM AA, and corresponding mixtures.

was applied to record the current responses. From the results in Table 2, it can be seen that the results of glucose detection in serum samples agreed well with the values obtained from the hospital-used instrument, and the relative standard deviation (RSD) of determination was below 4%, which implied the good accuracy of glucose.

Table 2. Glucose Determination in the Human Blood Serum Samples[a]

sample	measured by the hospital-used instrument (mM)	measured by the hospital-used instrument (mM)	RSD (%)
1	1.16	1.08	2.82
2	1.27	1.33	3.12
3	1.88	1.79	3.33
4	1.92	1.98	3.91

[a]The average value of five duplicate determinations for each sample by the graphene-encapsulated Cu nanoparticle electrode.

3. CONCLUSIONS

In summary, we have successfully developed an electrostatic self-assembly route for the fabrication of composites of Cu nanoparticles encapsulated in graphene shells. The obtained Cu@RGO composites showed excellent oxidation resistance ability than that of bare Cu and RGO/Cu composites because graphene shells can effectively protect the Cu core from oxidation. Compared with bare Cu and RGO/Cu composites, the as-prepared Cu@RGO composite exhibited better electrocatalytic activity toward glucose oxidation, which showed a broad linearity of 1 μM to 2 mM with a relatively low detection limit of 0.34 μM (S/N = 3). This could be attributed to the strong synergistic interaction between the Cu core and graphene shell, improved large surface area, and carrier transport efficiency, arising from the graphene encapsulation. Furthermore, the obtained Cu@RGO composites showed a long-term stability, great reproducibility, and excellent sensitivity (150 μA mM^{-1} cm^{-2}). Therefore, we believe that this synthesis method can be extended to other metal/graphene core−shell structure composites and Cu@RGO can be considered as a potential electrode for glucose sensors in the future.

4. METHODS

4.1. Materials. All of the chemicals were of analytical grade and used without any further purification. Graphene oxide (GO) was purchased from Nanjing XFNANO Materials Tech Co., Ltd. $NaH_2PO_2{\cdot}H_2O$ was obtained from Shanghai Chemical Reagent Co. The Cu nanocomposites and Cu-decorated graphene composites were fabricated by the chemical reduction method, which has been discussed in detail in our previous research.[17] All aqueous solutions were freshly prepared with ultrapure water (18 MΩ cm resistance, Millipore).

4.2. Preparation of Cu@RGO. Figure 1 shows the schematic illustration of the synthesis of Cu@RGO composites by the electrostatic self-assembly method. The negatively charged GO suspension was added into positively charged Cu solution and then the graphene-encapsulated Cu composites were obtained after adding the reducing agent. In a typical process, first, the obtained Cu nanoparticles (50 mg) were dispersed into ultrapure water (100 mL) via ultrasonication, followed by APTES (0.3 mL) addition into it. Next, the mixture was ultrasonically treated, magnetically stirred, and maintained at 60 °C for 4 h and then refluxed at 100 °C for 24 h. After that, the resulting suspension was washed with ultrapure water by filtration and dried at 50 °C in vacuum for 24 h. Subsequently, the dried APTES-modified Cu composites were dissolved into ultrapure water and then gradually into GO solution (20 mL, 1 mg mL^{-1}), which was obtained by ultrasonication for an hour and centrifugation five times. After magnetic stirring, the reducing agent ($NaH_2PO_2{\cdot}H_2O$, 0.1 g) was added into this solution to reduce GO to RGO. Finally, the mixture was centrifuged to obtain core−shell Cu@RGO nanoparticles.

4.3. Material Characterization. Atomic force microscopy (AFM, AXIS ULTRA DLD), scanning electron microscopy (SEM, JEOL, 7600F), and transmission electron microscopy (TEM, JEOL, 2100F) were employed to investigate the microstructure and morphology of GO and graphene. Raman spectroscopy spectra were recorded on a Senterra R200-L Raman system with an argon-ion (532 nm) laser source. Fourier transform infrared (FTIR) spectra were recorded by an EQUINOX55 FTIR spectrometer with KBr as the reference. X-ray photoelectron spectra (XPS) were recorded by employing Kratos AXIS Ultra X-ray with an Al Kα X-ray source ($h\nu$ = 1486.6 eV). X-ray power diffraction patterns were obtained by a Rigaku Ultima IV X-ray diffractometer with a scanning rate of 5° min^{-1} (Cu Kα radiation, 40 kV).

4.4. Electrochemical Measurements. Cyclic voltammetry (CV) and differential pulse voltammetry (DPV) were conducted on a CHI 660D electrochemical workstation using a conventional three-electrode system, where a saturated calomel electrode (SCE) and a platinum wire were used as the reference electrode and counter electrode, respectively. The as-prepared Cu@RGO and referential sample composite-modified glassy carbon electrodes (GCE) served as working electrodes. Nifion (perfluoridinghanated sulfonate ionomer), due to its easy fabrication, high chemical stability, and good biocompatibility, was used as a protective and selective coating material in this work. The electrocatalytic activity of as-prepared composites was assessed in an electrolyte of 0.1 M NaOH solution in the presence of 2 mM glucose by the CV technique from −0.2 to 1.0 V with a scan rate of 100 mV s^{-1}. DPV was applied to record the responsive signal of sensors.

DOI: 10.1021/acsomega.7b01197
ACS Omega 2018, 3, 3420−3428

The parameters were optimized as follows: potential range from −0.60 to 0.80 V (vs SCE), step potential 0.004 V, modulation amplitude 0.05 V, and modulation time 0.05 s. All tests were performed at room temperature (25 °C).

■ ASSOCIATED CONTENT

Supporting Information

The Supporting Information is available free of charge on the ACS Publications website at DOI: 10.1021/acsomega.7b01197.

Characterization of GO sheets, the size distribution of GO sheets, the mechanism for the oxidation of glucose on the Cu@RGO electrode; and CV curves of the Cu@RGO electrode in NaOH electrolyte (PDF)

■ AUTHOR INFORMATION

Corresponding Authors

*E-mail: anodic@sjtu.edu.cn. Tel: +86 02134203812. Fax: +86 021 34202749 (L.L.).

*E-mail: wuzhong2319@163.com (Z.W.).

ORCID

Lei Liu: 0000-0001-9244-1118

Notes

The authors declare no competing financial interest.

■ ACKNOWLEDGMENTS

We gratefully acknowledge the Major State Basic Research Development Program of China (973 Program) (No. 2014CB046701), National Natural Science Foundation of China (Nos. 51601114 and 51771117) and Collaborative Innovation Center for Advanced Ship and deep-Sea Exploration.

■ REFERENCES

(1) Wei, C. T.; Li, X.; Xu, F. G.; et al. Metal organic framework-derived anthill-like Cu@carbon nanocomposites for nonenzymatic glucose sensor. *Anal. Methods* **2014**, *6*, 1550−1557.

(2) Balakrishnan, S. R.; Hashim, U.; Letchumanan, G. R.; et al. Development of highly sensitive polysilicon nanogap with APTES/GOx based lab-on-chip biosensor to determine low levels of salivary glucose. *Sens. Actuators, A* **2014**, *220*, 101−111.

(3) Luo, J.; Jiang, S.; Zhang, H.; Jiang, J.; Liu, X. A novel non-enzymatic glucose sensor based on Cu nanoparticle modified graphene sheets electrode. *Anal. Chim. Acta* **2012**, *709*, 47−53.

(4) Huang, J. W.; He, Y. Q.; Jin, J.; Li, Y. R.; Dong, Z. P.; Li, R. A novel glucose sensor based on MoS2 nanosheet functionalized with Ni nanoparticles. *Electrochim. Acta* **2014**, *136*, 41−46.

(5) Wang, L.; Lu, X.; Wen, C.; et al. One-step synthesis of Pt−NiO nanoplate array/reduced graphene oxide nanocomposites for non-enzymatic glucose sensing. *J. Mater. Chem. A* **2015**, *3*, 608−616.

(6) Wang, L.; Zhang, Q.; Chen, S.; et al. Electrochemical sensing and biosensing platform based on biomass-derived macroporous carbon materials. *Anal. Chem.* **2014**, *86*, 1414−1421.

(7) Wang, L.; Yu, J.; Zhang, Y.; Yang, H.; Miao, L.; Song, Y. Simple and Large-Scale Strategy to Prepare Flexible Graphene Tape Electrode. *ACS Appl. Mater. Interfaces* **2017**, *9*, 9089−9095.

(8) Wang, L.; Lu, X.; Ye, Y.; Sun, L.; Song, Y. Nickel-cobalt nanostructures coated reduced graphene oxide nanocomposite electrode for nonenzymatic glucose biosensing. *Electrochim. Acta* **2013**, *114*, 484−493.

(9) Xu, W.; Dai, S.; Wang, X.; et al. Nanorod-aggregated flower-like CuO grown on a carbon fiber fabric for a super high sensitive non-enzymatic glucose sensor. *J. Mater. Chem. B* **2015**, *3*, 5777−5785.

(10) Chang, G.; Shu, H.; Huang, Q.; et al. Synthesis of highly dispersed Pt nanoclusters anchored graphene composites and their application for non-enzymatic glucose sensing. *Electrochim. Acta* **2015**, *157*, 149−157.

(11) Wang, S.; Huang, X.; He, Y.; et al. Synthesis, growth mechanism and thermal stability of copper nanoparticles encapsulated by multi-layer graphene. *Carbon* **2012**, *50*, 2119−2125.

(12) Chen, C.-C.; Lin, C.-L.; Chen, L.-C. Functionalized Carbon Nanomaterial Supported Palladium Nano-Catalysts for Electrocatalytic Glucose Oxidation Reaction. *Electrochim. Acta* **2015**, *152*, 408−416.

(13) Shu, H.; Chang, G.; Su, J.; et al. Single-step electrochemical deposition of high performance Au-graphene nanocomposites for nonenzymatic glucose sensing. *Sens. Actuators, B* **2015**, *220*, 331−339.

(14) Babu, T. G. S.; Ramachandran, T.; Nair, B. Single step modification of copper electrode for the highly sensitive and selective non-enzymatic determination of glucose. *Microchim. Acta* **2010**, *169*, 49−55.

(15) Huo, H.; Guo, C.; Li, G.; Han, X.; Xu, C. Reticular-vein-like Cu@Cu2O/reduced graphene oxide nanocomposites for a non-enzymatic glucose sensor. *RSC Adv.* **2014**, *4*, 20459−20465.

(16) Kim, C.; Lee, G.; Rhee, C.; Lee, M. Expeditious low-temperature sintering of copper nanoparticles with thin defective carbon shells. *Nanoscale* **2015**, *7*, 6627−6635.

(17) Zhang, Q.; Wu, Z.; Xu, C.; Liu, L.; Hu, W. Temperature-driven growth of reduced graphene oxide/copper nanocomposites for glucose sensing. *Nanotechnology* **2016**, *27*, No. 495603.

(18) Zeng, T.; Zhang, X. L.; Ma, Y. R.; Niu, H. Y.; Cai, Y. Q. A novel Fe 3O 4-graphene-Au multifunctional nanocomposite: Green synthesis and catalytic application. *J. Mater. Chem.* **2012**, *22*, 18658−18663.

(19) Yue, W.; Lin, Z.; Jiang, S.; Yang, X. Preparation of graphene-encapsulated mesoporous metal oxides and their application as anode materials for lithium-ion batteries. *J. Mater. Chem.* **2012**, *22*, 16318−16323.

(20) Yang, X.; Fan, K.; Zhu, Y.; et al. Tailored graphene-encapsulated mesoporous Co3O4 composite microspheres for high-performance lithium ion batteries. *J. Mater. Chem.* **2012**, *22*, 17278−17283.

(21) Sarno, M.; Cirillo, C.; Ciambelli, P. Selective graphene covering of monodispersed magnetic nanoparticles. *Chem. Eng. J.* **2014**, *246*, 27−38.

(22) Shao, D.; Yu, M.; Sun, H.; Hu, T.; Lian, J.; Sawyer, S. High responsivity, fast ultraviolet photodetector fabricated from ZnO nanoparticle-graphene core-shell structures. *Nanoscale* **2013**, *5*, 3664−3667.

(23) Zhang, J.; Zhu, Z.; Tang, Y.; Feng, X. Graphene encapsulated hollow TiO2 nanospheres: Efficient synthesis and enhanced photocatalytic activity. *J. Mater. Chem. A* **2013**, *1*, 3752−3756.

(24) Yue, H.; Wang, S.; Yang, Z.; Li, Q.; Lin, S.; He, D. Ultra-thick porous films of graphene-encapsulated silicon nanoparticles as flexible anodes for lithium ion batteries. *Electrochim. Acta* **2015**, *174*, 688−695.

(25) Hang, L.; Zhao, Y.; Zhang, H.; et al. Copper nanoparticle@graphene composite arrays and their enhanced catalytic performance. *Acta Mater.* **2016**, *105*, 59−67.

(26) Wang, C.; Zhai, P.; Zhang, Z.; et al. Nickel catalyst stabilization via graphene encapsulation for enhanced methanation reaction. *J. Catal.* **2016**, *334*, 42−51.

(27) Ding, D.; Song, Z. L.; Cheng, Z. Q.; et al. Plasma-assisted nitrogen doping of graphene-encapsulated Pt nanocrystals as efficient fuel cell catalysts. *J. Mater. Chem. A* **2014**, *2*, 472−477.

(28) Akhavan, O. Photocatalytic reduction of graphene oxides hybridized by ZnO nanoparticles in ethanol. *Carbon* **2011**, *49*, 11−18.

(29) Zhang, M.; Wang, Y.; Jia, M. Three-Dimensional Reduced Graphene Oxides Hydrogel Anchored with Ultrafine CoO Nanoparticles as Anode for Lithium Ion Batteries. *Electrochim. Acta* **2014**, *129*, 425−432.

(30) Zhou, Y.; Liu, Q.; Liu, D.; et al. Carbon-coated MoO2 dispersed In Three-dimensional graphene aerogel for lithium-ion battery. *Electrochim. Acta* **2015**, *174*, 8−14.

(31) Zhang, Y.; Chang, G.; Liu, S.; et al. Microwave-assisted, environmentally friendly, one-pot preparation of Pd nanoparticles/

DOI: 10.1021/acsomega.7b01197
ACS Omega 2018, 3, 3420−3428

graphene nanocomposites and their application in electrocatalytic oxidation of methanol. *Catal. Sci. Technol.* **2011**, *1*, 1636.
(32) Zhang, G.; Zhou, Y.; Chen, J.; Yang, F. Potentiostatic-Potentiodynamic Reduction Synthesis of Anthraquinone Functionalized Graphene for Oxygen Reduction in Alkaline Medium. *Int. J. Electrochem. Sci.* **2012**, *7*, 11323−11337.
(33) Moghal, J.; Wu, Y. M. A.; Warner, J. H. Mechanical response of few-layer graphene films on copper foils. *Scr. Mater.* **2012**, *67*, 273−276.
(34) Wang, Y.; Zhao, Y.; Bao, T.; Li, X.; Su, Y.; Duan, Y. Preparation of Ni-reduced graphene oxide nanocomposites by Pd-activated electroless deposition and their magnetic properties. *Appl. Surf. Sci.* **2012**, *258*, 8603−8608.
(35) Yan, H.; Zhao, T.; Li, X.; Hun, C. Detonation Synthesis and Friction-Wear Test of Carbon-Encapsulated Copper Nanoparticles. *J. Inorg. Organomet. Polym. Mater.* **2015**, *25*, 1569−1575.
(36) Chu, K.; Jia, C. Enhanced strength in bulk graphene-copper composites. *Phys. Status Solidi A* **2014**, *211*, 184−190.
(37) Liu, J.; Yu, B.; Zhang, Q.; et al. Synthesis and magnetic properties of Fe3C-C core-shell nanoparticles. *Nanotechnology* **2015**, *26*, No. 085601.
(38) Rakibuddin, M.; Ananthakrishnan, R. Effective photocatalytic dechlorination of 2,4- dichlorophenol by a novel graphene encapsulated ZnO/Co3O4 core−shell hybrid under visible light. *Photochem. Photobiol. Sci.* **2016**, *15*, 86−98.
(39) Zhai, J.; Sun, L.; Yu, H.; et al. A facile approach of fabricating graphene-encapsulated ZnO microspheres and their synergic effect on photocatalytic performance. *J. Nanopart. Res.* **2014**, *16*, 2433.
(40) Fan, Z.; Liu, B.; Liu, X.; et al. A flexible and disposable hybrid electrode based on Cu nanowires modified graphene transparent electrode for non-enzymatic glucose sensor. *Electrochim. Acta* **2013**, *109*, 602−608.
(41) Wang, B.; Wu, Y.; Chen, Y.; Weng, B.; Li, C. Flexible paper sensor fabricated via in situ growth of Cu nanoflower on RGO sheets towards amperometrically non-enzymatic detection of glucose. *Sens. Actuators, B* **2017**, *238*, 802−808.
(42) Prathap, M. U. A.; Pandiyan, T.; Srivastava, R. Cu nanoparticles supported mesoporous polyaniline and its applications towards non-enzymatic sensing of glucose and electrocatalytic oxidation of methanol. *J. Polym. Res.* **2013**, *20*, 83.
(43) Yang, H.; Hou, Z.; Zhou, N.; He, B.; Cao, J.; Kuang, Y. Graphene-encapsulated SnO2 hollow spheres as high-performance anode materials for lithium ion batteries. *Ceram. Int.* **2014**, *40*, 13903−13910.
(44) Yang, T.; Xu, J.; Lu, L.; et al. Copper nanoparticle/graphene oxide/single wall carbon nanotube hybrid materials as electrochemical sensing platform for nonenzymatic glucose detection. *J. Electroanal. Chem.* **2016**, *761*, 118−124.
(45) Jiang, D.; Liu, Q.; Wang, K.; et al. Enhanced non-enzymatic glucose sensing based on copper nanoparticles decorated nitrogen-doped graphene. *Biosens. Bioelectron.* **2014**, *54*, 273−278.
(46) Wang, Q.; Wang, Q.; Li, M.; Szunerits, S.; Boukherroub, R. Preparation of reduced graphene oxide/Cu nanoparticle composites through electrophoretic deposition: Application for nonenzymatic glucose sensing. *RSC Adv.* **2015**, *5*, 15861−15869.
(47) Luo, J.; Zhang, H.; Jiang, S.; Jiang, J.; Liu, X. Facile one-step electrochemical fabrication of a non-enzymatic glucose-selective glassy carbon electrode modified with copper nanoparticles and graphene. *Microchim. Acta* **2012**, *177*, 485−490.
(48) Wang, X.; Hu, C.; Liu, H.; Du, G.; He, X.; Xi, Y. Synthesis of CuO nanostructures and their application for nonenzymatic glucose sensing. *Sens. Actuators, B* **2010**, *144*, 220−225.
(49) Jin, J.; Liu, W.; Deng, S.; Han, Y.; Cai, Y.; Hui, G. A non-enzyme electrochemical qualitative and quantitative analyzing method for glucose, D-fructose, and sucrose utilizing Cu foam material. *Electrochim. Acta* **2015**, *153*, 594−601.
(50) Yang, J.; Zhang, W.-D.; Gunasekaran, S. An amperometric non-enzymatic glucose sensor by electrodepositing copper nanocubes onto vertically well-aligned multi-walled carbon nanotube arrays. *Biosens. Bioelectron.* **2010**, *26*, 279−284.
(51) Luo, J.; Jiang, S.; Zhang, H.; Jiang, J.; Liu, X. A novel non-enzymatic glucose sensor based on Cu nanoparticle modified graphene sheets electrode. *Anal. Chim. Acta* **2012**, *709*, 47−53.
(52) Kang, X.; Mai, Z.; Zou, X.; Cai, P.; Mo, J. A sensitive nonenzymatic glucose sensor in alkaline media with a copper nanocluster/multiwall carbon nanotube-modified glassy carbon electrode. *Anal. Biochem.* **2007**, *363*, 143−150.
(53) Wu, H. X.; Cao, W. M.; Li, Y.; et al. In situ growth of copper nanoparticles on multiwalled carbon nanotubes and their application as non-enzymatic glucose sensor materials. *Electrochim. Acta* **2010**, *55*, 3734−3740.
(54) Huang, J.; Dong, Z.; Li, Y.; et al. High performance non-enzymatic glucose biosensor based on copper nanowires−carbon nanotubes hybrid for intracellular glucose study. *Sens. Actuators, B* **2013**, *182*, 618−624.
(55) Zhuang, Z.; Su, X.; Yuan, H.; Sun, Q.; Xiao, D.; Choi, M. M. An improved sensitivity non-enzymatic glucose sensor based on a CuO nanowire modified Cu electrode. *Analyst* **2008**, *133*, 126−132.
(56) Zheng, B.; Liu, G.; Yao, A.; et al. A sensitive AgNPs/CuO nanofibers non-enzymatic glucose sensor based on electrospinning technology. *Sens. Actuators, B* **2014**, *195*, 431−438.

DOI: 10.1021/acsomega.7b01197
ACS Omega 2018, 3, 3420−3428